Assessing microbial growth monitoring methods for challenging strains and cultures

Damon Brown[1], Raymond J. Turner[1*]

[1] Biological Sciences, University of Calgary, Calgary, Alberta, Canada

* Corresponding author

E-mail: turnerr@ucalgary.ca (RT)

Abstract

This is a paper focusing on the comparison of growth curves using field relevant testing methods and moving away from colony counts. Challenges exist to explore antimicrobial growth of fastidious strains, poorly culturable bacterial and bacterial communities of environmental interest. Thus, various approaches have been explored to follow bacteria growth that can be an efficient surrogate for classical optical density or colony forming unit measurements.

Here we tested optical density, ATP assays, DNA concentrations and 16S rRNA qPCR as means to monitor pure culture growth of six different species including *Acetobacterium woodii, Bacillus subtilis, Desulfovibrio vulgaris, Geoalkalibacter subterraneus, Pseudomonas putida* and *Thauera aromatica*. Optical density is and excellent, rapid monitoring method of pure culture planktonic cells but cannot be applied to environmental or complex samples. ATP assays provide rapid results but conversions to cell counts may be misleading for different species. DNA concentration is a very reliable technique which can be used for any sample type and provides genetic materials for downstream applications. qPCR of the 16S rRNA gene is a widely applicable technique for monitoring microbial cell concentrations but is susceptible to variation between replicates. DNA concentrations were found to correlate the best with the other three assays and provides the advantages of rapid extraction, consistency between replicates and potential for downstream analysis, DNA concentrations is determined to be the best universal monitoring method for complex environmental samples.

Introduction

Assessing growth is fundamental to nearly all microbial studies. On the surface this is an easy procedure done in introductory courses worldwide [1]. However, it turns out this routine experiment is

not as trivial as one thinks. For easily culturable aerobic species, the process is relatively simple as the growth medium need only contain the appropriate carbon sources and essential nutrients to culture the typical well studied model microbes. After the appropriate growth medium has been selected, direct cell counting on agar plates can be performed for accurate quantification providing colony forming units (CFU) or viable cell count (VCC) values. However, it has become apparent that this method restricts the scope of species possible for study and cannot but use to study complex environments [2–4]. For more rapid analysis, optical density (OD) is evaluating the scatting of light by cells, either using the classical Klett meter or an absorption spectrometer set to 550 or 600 nm. This however is also limiting due to suspended material in various growth media and the inability to decipher living vs dead vs flocculation from extracellular polysaccharides. Additionally, size and shape of cells effect scattering and can lead to misinterpretation of cell numbers. Related rapid assays includes color dependant activity assays (colloquially known as bug bottles or biological activity reaction test (BART) bottles [5]), microscopy (grid cell counting and live dead staining) [6–8], dyes such as crystal violet or 5-(4,6-dichlorotriazinyl) aminofluorescein (DTAF) for total biomass staining [9,10] or metabolic dyes to determine actively respiring cells such as 5-cyano-2,3-ditolyl tetrazolium chloride (CTC) [10]. Fluorescent *in situ* hybridization (FISH) is a target-specific approach which relies on a fluorescent reporter attached to a nucleic probe to determine the presence and abundance of the target sequence. This can be used for total or genera-specific cell enumeration when targeting a gene such as 16S rRNA [11,12]. Now in our genomics era, 16S rRNA quantification using quantitative PCR (qPCR) is gaining popularity with [13] or without sequencing databases [14,15].

For anaerobes, accurate cell enumeration becomes increasingly more difficult as different anaerobes will require different oxidation-reduction potentials (ORP) to thrive; ≤ -100 mV for obligate anaerobes [16] and ≤ -330 mV for strict anaerobes [17]. Following the improved Hungate culturing

technique of anaerobes [18,19], it is possible to isolate and enumerate pure culture anaerobes [20,21] but direct microscopy and fluorescent in-situ hybridization (FISH) and more common enumeration techniques [22–25]. A review of anaerobic culturing and quantification is available elsewhere [26]. In many instances, the difficulty of culturing anaerobes forces researchers to choose indirect methods to assess growth and activity, such as rates of substrate consumption or end-product production, where an easily quantified chemical is sampled and measured at time points in favor of actual cell counting [27,28]. The rate of consumption or production relates to cell growth through the Monod equation [29]. It should be noted that there is a distinction between cell counting and microbial activity, and the need to monitor one or the other or both depends on the research, environmental, industrial, or medical question being asked.

The above exemplify the issues of accurate quantification of aerobic and anaerobic pure cultures. This task becomes exponentially more difficult when considering environmental samples which have diverse, unspecified microbial species present. In such examples, highly specific monitoring methods are no longer viable to determine accurate cell counts so general techniques must be used. The typical trade off when transitioning to general monitoring from selective is the loss of specificity (e.g. the presence of a specific pathogen) for the gain of total cell counts. General quantification is an important technique for the monitoring of hydrocarbon remediation efforts and wastewater treatments [30,31].

In this study, we take the opportunity to review the various methods to evaluate microbial growth. We then compare select testing methods used in environmental/industrial applications. From our groups interest we will look at ATP levels and 16S rRNA qPCR which are being adapted in in oil and gas industries in western Canada. These are then compared to traditional OD_{600} and qPCR targeting 16S rRNA to determine how reliable, complementary and efficient these differing methods are.

Materials and methods

Cultures and media

Six pure cultures were used in this study acquired from DSMZ. The cultures are *Acetobacterium woodii* (DSM 1030), *Bacillus subtilis* (DSM 10), *Desulfovibrio vulgaris* (DSM 644), *Geoalkalibacter subterraneus* (DSM 29995), *Pseuodomonas putida* (DSM 291), and *Thauera aromatica* (DSM 6984). Each of the chosen species has a representative genome sequenced on NCBI and their details are in Table 1. Pure cultures were recovered from -70 °C freezer stocks (10% glycerol) into the suggested media (DSM medium 135, medium 1, medium 63, medium 1249, medium 1a, and medium 586, respectively) prepared in 20 mL aliquots and sealed in 26 mL Hungate tubes with anaerobic headspaces (either N_2 or N_2/CO_2). Fresh media tubes were inoculated with the freezer recovery culture and incubated at the recommended temperatures for 7 days, then fresh media tubes were inoculated in triplicate with a 10% inoculant.

Table 1. Representative sequenced genome chosen and identified 16S rRNA copy numbers

Species and strain	NCBI accession number	Genome length (bp)	16S rRNA copy number*
Acetobacterium woodii DSM 1030	CP002987.1	4044777	5
Bacillus subtilis subtilis 168	CP010052	4215619	10
Desulfovibrio vulgaris Miyazaki F	CP001197.1	4040304	4
Geoalkalibacter subterraneus Red1	CP010311	3475523	4
Pseudomonas putida KT2440	AE015451.2	6181873	7
Thauera aromatica MZ1T	CP001281.2	4496212	4

*Counted manually from NCBI sequences

Sampling and testing

Once inoculated, the fresh cultures were sampled in a time course for testing. At each point, sterile syringe and needles were used to aseptically remove 2 mL. This aliquot was split, 1 mL used to measure OD_{600} in a Hitachi U-2000 Spectrophotometer (reference sample was uninoculated media) and was then recovered and used for DNA extraction in the MPBio FastDNA® Spin Kit. The DNA concentration was measured using Invitrogen Qubit™ fluorometer and the Quant-iT™ dsDNA HS assay kit. Following quantification, DNA was cleaned using the OneStep™ PCR inhibitor removal kit (Zymo Research) prior to being used in quantitative PCR (qPCR). The other 1 mL was consumed to measure ATP using the LifeCheck ATP test kits (OSP).

Quantitative PCR

qPCR was done targeting the 16S rRNA gene, specifically 515-809 (variable region 4) using modified primers from Caporaso *et al.* [32]. Primer sequences are provided in Table 2. Starting quantification was determined using synthetic gBlocks purchased from IDT (IDTdna.com) at concentrations of 10^{8-3} copies/µL. The gBlock used contained the target 16S rRNA sequence flanked by two multidrug resistance genes (for use in other studies), separated by sequences of ten thymines. The entire gBlock sequence is provided in Table 3. Reaction mixtures were prepared to a total volume of 20 µL, with 10 µL PowerUp™ SYBR™ Green 2X Master Mix (appliedbiosystems), 1.2 µL 10 µM 515_F, 0.6 µL 10 µM 806_R, 6.2 µL nuclease free water and 2 µL DNA template. Thermocycling was performed in a BioRad CFX96 Real-Time PCR System with the following protocol: 50 °C – 2 minutes, 95 °C – 2 minutes followed by 50 cycles of 95 °C for 45 seconds, 55 °C for 30 seconds and 72 °C for 45 seconds.

Table 2. Primer sequences used in quantitative PCR

Primer name	Sequence (5'-3')	Melting Temperature (°C)
519_F	CAG C**M**G CCG CGG TAA	57.6
806_R	GGA CTA C**HV** GGG T**W**T CTA AT	50.7

Nucleotide codes: H = A/C/T; M = A/C; V = A/C/G; W = A/T

Table 3. gBlock DNA sequence

gBlock DNA sequence (5'-3') (Multidrug resistance efflux pump gene A - Universal 16S rRNA – Multidrug resistance efflux pump gene A)
Multidrug resistance gene A amplicon **TTTTTTTTTT** GTG CCA GCA GCC GCG GTA ATA CAG AGG GTG CAA GCG TTA ATC GGA ATT ACT GGG CGT AAA GCG CGC GTA GGT GGT TTG TTA AGT TGG ATG TGA AAG CCC CGG GCT CAA CCT GGG AAC TGC ATC CAA AAC TGG CAA GCT AGA GTA CGG TAG AGG GTG GTG GAA TTT CCT GTG TAG CGG TGA AAT GCG TAG ATA TAG GAA GGA ACA CCA GTG GCG AAG GCG ACC ACC TGG ACT GAT ACT GAC ACT GAG GTG CGA AAG CGT GGG GAG CAA ACA GGA TTA GAT ACC CTG GTA GTC C **TTTTTTTTTT** Multidrug resistance gene B amplicon

Cell count calculations

For direct comparison, cell counts, such as they are inferred and calculated for each method, were calculated. OD_{600} was not converted to cell count equivalent in presented data. The chosen ATP method produces relative light units (RLU) per milliliter, as 1 mL of each culture was used in the assay, the microbial equivalents (ME) produced are used directly as calculated cell counts. DNA concentrations were converted into a cell count proxy using the assumption of 2 fg of DNA per cell, taken as an average from values reported by Bakken and Olson, 1989 [33]. To convert qPCR values into cell counts, the copies of 16S rRNA

genes per µL were converted to copies mL^{-1}, then divided by the 16S rRNA gene copies counted in the NCBI sequenced genomes (see Table 1).

Results

Optical Density

Growth of each culture was monitored using OD_{600} (reference media was each species' uninoculated media). The results of the time course sampling using OD_{600} for each species is shown in Figure 1, panels A-F. It is important to note the time courses and the OD_{600} scales are all unique for each species. *A. woodii, G. subterraneus* and *P. putida* (Fig. 1A, D, and E) followed a typical sigmoidal growth curve although their lag phases varied in length. *B. subtilis* (Fig. 1B) showed a diauxic growth curve, likely a result of the media not being fully anoxic but containing an anaerobic headspace. *D. vulgaris* is a steady increase over the course of the 48-hour testing period rather than a sharp sigmoidal curve (Fig. 1C). Is it interesting to note that the growth trend is still observable, though muted, in the *D. vulgaris* culture despite having readings above 1.0 (Figure 1.C). *T. aromatica* (Fig. 1F) shows a modified sigmoidal curve, however the peak occurs following the log phase before dipping then and plateauing into the stationary phase.

A formula was created by Kim et al. (2012) studying *Pseudomonas aeruginosa* which found the following relation of OD_{600} to colony forming units (CFU):

Colony forming units (CFU/mL) = $2 \times 10^8 * OD_{600} + 4 \times 10^6$ [34]

It is noted that this formula should be confirmed by plating cells at unique OD_{600} values and validating the formula for each pure culture. It is acknowledged that the differences in culture turbidity of the six species used in this study and the inability to grow all six on plated media means converting OD_{600} to CFU values will be an inaccurate conversion, but this was still done to maintain uniformity between datasets and to highlight the issue of using such conversion factors without confirming and modifying the equation empirically for each species. Thus we used this to convert values for time zero, a time point to represent the mid log phase and a time point to represent the stationary phase, which are reported in Table 5.

Figure 1. Optical density time course for each species. OD_{600} time course of A) *A. woodii,* B) *B. subtilis,* C) *D. vulgaris,* D) *G. subterraneus,* E) *P. putida* and F) *T. aromatica*. Blue lines are the species growth curves (n=3), orange line is the inoculant value.

Cellular ATP Levels

ATP measurements were converted into microbial equivalents (ME) according to the manufacturer's protocol using the relative light units (RLU) from manufacturer's luminometer as in equation (1).

$$\text{Microbial equivalents (ME/mL)} = \frac{(sample\ RLU - blank\ RLU)}{standard\ RLU} * \frac{10{,}000}{Sample\ size\ (1\ mL)} * 1000 \quad (1)$$

Calculated ME are plotted in Figure 2. Data is not displayed in log scale to better illustrate fluctuations in data trends. *A. woodii* shows a gradual increase in ME/mL between time 0 and 24 hours, going from 8.77 x 10^7 ME/mL (T = 0) to 7.48 x 10^8 ME/mL at 24 hours (Fig. 2A). There was a sharp increase after this point to 1.45 x 10^9 ME/mL at 32 hours, after which readings remained relatively stable at 1.33 x 10^9 ME/mL until the final time point of 48 hours. *B. subtilis* readings were less constant, reaching peak values at 13 hours (2.64 x 10^8 ME/mL) before dipping to 8.26 x 10^7 ME/mL at 24 hours and subsequently recovering to 2.47

x 10^8 ME/mL at 37 hours. After this point readings gradually decrease to 1.58 x 10^8 ME/mL at the final timepoint of 48 hours (Fig. 2B). *D. vulgaris* ME/mL readings did not follow a typical sigmoidal growth curve, rather they peaked at 31 hours (3.01 x 10^8 ME/mL) before declining to 1.56 x 10^8 ME/mL at 44 hours where it remained relatively stable for the remainder of the time points (Fig. 2C). *G. subterraneus* had a similar trend in ME, with the peak occurring at 12 hours (2.41 x 10^8 ME/mL) before decreasing to 6.30 x 10^7 ME/mL at the final time point (T = 36 hours) (Fig. 2D). *P. putida* followed a sigmoidal curve with a short lag phase in the first two hours (4.12 x 10^7 ME/mL at T = 0 to 1.17 x 10^8 at T = 2 hours) before reaching 5.77 x 10^8 ME/mL at 6 hours, after which it gradually increased for the remainder of the growth curve, reaching 9.89 x 10^8 ME/mL at T = 49.5 hours (Fig. 2E). *T. aromatica* followed a sigmoidal curve with a lag phase between 0 and 8 hours (5.81 x 10^7 ME/mL and 9.15 x 10^7 ME/mL, respectively) before increasing to 6.29 x 10^8 ME/mL at T = 32 hours where it remains until T = 44 hours, after which it drops to 4.41 x 10^8 ME/mL at T = 48 hours (Fig. 2E).

An interesting observation is the ATP values of the T = 0 hour time point is higher or near to the value of the inoculant, as in the case of *G. subterraneus* (Fig. 2D), *T. aromatica* (Fig. 2F) and *P. putida* (Fig. 2E). It is hypothesized this is a result of the inoculant culture being in stationary and/or death phase at the time of inoculation, lowering the ATP readings, but the cultures were capable of rapidly activating their metabolism again when exposed to fresh media. This highlights that ATP levels reflect metabolizing bacteria concentration only.

Figure 2. Microbial equivalents time course as determined using luciferase-based ATP assay for each species. Microbial equivalents per milliliter calculated for a time course of A) *A. woodii,* B) *B. subtilis,* C) *D. vulgaris,* D) *G. subterraneus,* E) *P. putida* and F) *T. aromatica*. Blue lines are the species growth curves (n=3), orange line is the inoculant value.

DNA concentration

The DNA concentrations were measured from 1 mL aliquots sampled at each time point and are reported in Figure 3. *A. woodii* DNA concentrations follow a typical sigmoidal curve but peaked at the mid-point of the growth curve (24.9 µg/mL, T = 24 hours), after which the DNA concentration dipped slightly to 21.1 µg/mL at T= 28 hours then remained stable between 23.6 µg/mL and 27.5 µg/mL (Fig. 3A). *B. subtilis* DNA concentrations followed a similar trend as the OD_{600} and ATP, indicating a diauxic growth pattern (Fig. 3B), where DNA concentrations were at their highest at 24 and 48 hours (11.8 µg/mL and 12.0 µg/mL respectively). Between these time points the DNA concentrations dip to 7.2 µg/mL at 37 hours. *D. vulgaris* DNA concentrations followed more of a sigmoidal curve compared to the OD_{600} readings, possibly owing to the high scattering properties of the *D. vulgaris* media particulates minimizing the effect of the cells alone, as discussed above. DNA concentrations showed a lag phase between T = 0 hours and T = 19 hours, where concentrations varied between 1.7-2.7 µg/mL before increasing to 28.7 µg/mL at T = 31 hours (Fig. 3C). DNA concentrations peaked at 44 hours (37.0 µg/mL) before decreasing to 30.0 µg/mL at the final time point (T = 52.5 hours). *G. subterraneus* DNA concentrations followed a standard sigmoidal curve, nearly identical to the OD_{600} curve. The lag phase occurred between 0 and 8 hours, during which DNA concentrations were between 4.2-6.1 µg/mL before increasing up to 32.7 µg/mL at 24 hours and decreasing to 28.5 µg/mL at 32 hours (Fig. 3D). It should be noted DNA was not collected at the 36 hour time point due to lack of supplies, thus DNA concentrations could not be collected for the final time point. *P. putida* also exhibited a classic sigmoidal curve in the DNA concentrations as with the OD_{600} and ATP, but there is a shorter lag phase and a longer stationary phase (Fig. 3E) than is typical of a sigmoidal curve. The lag phase was between 0 and 2 hours (4.2 µg/mL and 8.9 µg/mL, respectively), then DNA concentrations increased to 63.9 µg/mL at 9 hours, then gradually increasing to 86.4 µg/mL by the final time point at 49.5 hours. *T. aromatica* DNA concentrations follow a gradual sigmoidal curve, lacking significant lag or stationary phases (Fig. 3F). The lag phase was between 0 and 8 hours (1.2 µg/mL and 3.2

219 µg/mL respectively), then a steady increase to 57.0 µg/mL by 48 hours, after which there was a slight
220 decline to 55.3 µg/mL at the last time point.

221 DNA concentrations were converted into a cell proxy estimation by assuming 2.0 fg DNA per cell
222 based on the average 1.6-2.4 fg/cell [33]. Converted cell proxy values for time zero, a time point
223 representative of mid log phase and a time point representative of the stationary phase are reported in
224 Table 5. An interesting point is that at all time points, even initial (0 hours), the calculated cell counts are
225 never below 10^8 cells/mL, and between initial time points and stationary phase, the calculated cell counts
226 increase by one or two orders of magnitude.

227 **Figure 3. DNA concentration time course for each species.** DNA concentrations in micrograms per
228 milliliter over a time course of A) *A. woodii,* B) *B. subtilis,* C) *D. vulgaris,* D) *G. subterraneus,* E) *P. putida*
229 and F) *T. aromatica* as measured by a Qubit fluorometer. Blue lines are the species growth curves (n=3),
230 orange line is the inoculant value.

231

232 qPCR of 16S rRNA

233 As with the ATP data, we have not plotted the qPCR data in log format. Each of the three biological
234 replicates collected at each timepoint were ran in duplicate on the thermocycler, raising the N value to
235 six. The 16S rRNA copies measured per µL are shown in Figure 4. A key point to highlight in all the trends
236 is an increase in the error bars, especially in the later time points of the graphs. The trends of the 16S
237 rRNA qPCR results followed the DNA concentrations for all species. The 16S rRNA copy numbers for *A.*
238 *woodii* showed the same lag phase as DNA between 0 and 8 hours, where copy numbers were between
239 7.23×10^5 copies/µL and 1.69×10^6 copies/µL. The counts increase to 1.64×10^7 copies/µL at 24 hours,
240 then dip slightly to 1.58×10^7 copies/µL before increasing again to 2.07×10^7 copies/µL at the final time

point of 48 hours (Fig. 4A). *B. subtilis* showed a lag phase up to 8 hours ($3.09 \times 10^5 – 8.85 \times 10^5$ copies/µL) before falling into the same diauxic growth curve seen in other monitoring methods. The initial increase peaked at 24 hours (1.11×10^7 copies/µL) before falling to 6.04×10^6 copies/µL at 37 hours and increasing again to 1.13×10^7 copies/µL at 48 hours (Fig. 4B). The lag phase of *D. vulgaris* occurred between 0 and 19 hours ($2.35 \times 10^6 – 4.04 \times 10^6$ copies/µL) before increasing to 3.99×10^7 copies/µL at 31 hours, where they remained relatively stable until 48 hours (3.63×10^7 copies/µL) (Fig. 4C). At this point, the *D. vulgaris* curve becomes skewed due to significant error bars on the final time point (T = 52.5 hours), owing to half the replicates (n = 3) reporting values an order of magnitude less than the other three replicates (1.52×10^8 copies/µL ± 1.16×10^8). The *G. subterraneus* growth curve shows a lag phase between 0 and 8 hours ($1.17 \times 10^7 – 1.72 \times 10^7$ copies/µL) before increasing to 5.38×10^7 copies/µL at 24 hours then decreasing to 4.70×10^7 copies/µL at 32 hours (Fig. 4D). As with the DNA concentrations, no DNA was available for the final time point (T = 36 hours) and therefore no values are reported. *P. putida* 16S rRNA copies/µL show a far less tidy sigmoidal curve compared to the other monitoring methods. The lag phase occurred between 0 and 2 hours ($3.00 \times 10^6 – 9.64 \times 10^6$ copies/µL) before it increased to 5.57×10^7 copies/µL at the start of stationary phase (T = 6 hours) (Fig. 4E). After T = 6 hours where other lines of evidence show a gradual increase into a plateau, the 16S rRNA data fluctuate between $3.36 \times 10^7 – 7.20 \times 10^7$ copies/µL with the peak values occurring at T= 24 hours (7.20×10^7 copies/µL). *T. aromatica* 16S rRNA copies/µL show a lag phase between 0 and 8 hours ($2.80 \times 10^6 – 6.79 \times 10^6$ copies/µL) before increasing to 9.57×10^7 copies/µL at 28 hours then enter stationary phase for the remainder of the growth curve, which increased slightly to 1.05×10^8 copies/µL at 48 hours (Fig. 4F).

Cell count equivalents for 16S qPCR readings are reported in Table 5 and were calculated using the unique 16S rRNA gene copy numbers (per cell) as reported in Table 1.

Figure 4. Quantitative PCR results targeting 16S rRNA of a time course for each species. 16S rRNA copies per microliter as detected by qPCR over a time course of A) *A. woodii,* B) *B. subtilis,* C) *D. vulgaris,* D) *G.*

265 *subterraneus,* E) *P. putida* and F) *T. aromatica*. Blue lines are the species growth curves (n=6, three
266 biological each with two technical replicates), orange line is the inoculant value.

267

268 Discussion

269 First let's take the opportunity to do a 'mini' review of cell quantitation (count) methods for
270 bacterial growth. In laboratory-based research, it is taken for granted the simplicity of assessing microbial
271 growth. This is typically performed using direct counting methods such as colony forming units (CFU)
272 plated on appropriate agar, where after each incubation each cell can be visualized as a unique colony on
273 the agar. Other metabolic or growth specific methods exist such as dilution series (colloquially known as
274 "bug bottles") [35] and bacteriological activity reaction test (BART) bottles [5], both of which produce a
275 colour change resulting from specific microbial growth and metabolism where the time until detectable
276 change (i.e. a change in the colour of the media) is used to approximate the initial microbiological cell
277 count. These are commercially available for sulfate reducing bacteria, acid producing bacteria, iron
278 reducing bacteria and others. All these methods are dependent on the culturability of the microbes in
279 question and are not applicable when the species in question cannot be cultured easily or conveniently.
280 Due to the nature of these techniques and their estimation of culturable microorganisms and not
281 quantitative enumeration, these techniques are more commonly used in industry where exact cell counts
282 are not required as opposed to scientific endeavours which typically require more precise counts.

283 During planktonic growth, optical density (OD) is frequently used as a rapid monitoring method
284 where the turbidity of the media is correlated to the cell density. If a sample or culture has high turbidity,
285 the effect of light scattering by the cells is diminished and the measured OD becomes too high to provide
286 a linear application of the Beer-Lambert law. Studies have shown that OD measurements to assess cell

counts are highly dependent on the spectrophotometer, wavelength, media type, growth stage, cell morphology and the presence and concentration of secreted compounds, and thus OD measurements should be taken as a proxy and not as concrete correlations [36]. Klett units are a similar means of determining cell concentrations using turbidity, where the turbidity of a liquid culture has been correlated to a colony forming unit value, and this is commonly done on a per strain basis via wavelength filters as part of this older tool [37,38]. Direct comparison of OD for different species is difficult due to changes in turbidity resulting from cell shape such as rod compared to coccoid and cell agglomeration to flocculation issues and thus not individual cell density which can lead to incorrect assumptions at the same OD. This will not pose an issue while studying a pure culture of known shape as comparisons are direct. However, for cross comparisons or for mixed cultures this becomes a significant issue and lowers the utility and accuracy of OD as a tool for growth measurement.

Moving away from the culture-dependant methods, dyes and stains can be used to visualize and semi-quantitatively measure growth. Crystal violet is used as a biofilm assessment assay [39] but Safranin has been found to be more reproducible [40]. These stains do not provide true cell counts but produce quantifiable biomass measurements, which depending on the research question posed is sufficient to monitor microbial growth.

Other, less direct methods exist which can approximate cell counts through quantification of other components such as key metabolites including ATP or major biochemical compositions such as protein concentration, DNA concentration, or lipid composition. Each of these techniques relies on an average quantity of the target molecule being present in each cell and have similar trends and limitations as DNA, where fluctuating concentrations may be a reflection of a specific stage of cellular division, but largely the absolutely concentrations are maintained at a steady state [41–43]. Lipids can also be used to determine growth rates by tracking the incorporation of heavy water into lipids using gas chromatography [44]. In the case of ATP, assays use an average quantity of ATP per cell based on *E. coli* where one *E. coli*

311 cell contains approximately 1 femtogram of ATP [45], while other studies have shown ATP concentrations
312 are stable throughout all growth rates, although exact ATP concentrations per cell were not calculated
313 [46]. These assumptions do not take into account periods of external stress (e.g. biocide exposure) or
314 temperature increases which may increase the intracellular ATP concentrations in response [47]. An
315 added benefit of these methods when considering non-defined environmental samples is that they are
316 only present in biochemically active cells, and free molecules do not survive for long outside of a living
317 cell. As such, in environmental samples these lines of evidence can be reasonably used to estimate total
318 biomass without having to consider the types or diversity of species present.

319 More advanced methods of quantifying the number of organisms present in complex samples
320 have arisen from molecular methods such as quantifying specific gene copy numbers including 16S rRNA
321 genes, housekeeping genes other species-specific marker genes. Many databanks exist which have
322 developed different 16S rRNA primer sets, each with their own biases towards detecting or omitting
323 certain microbial clades and are reviewed elsewhere [48–50]. Primer sets are often chosen if there is an
324 indication as to the types of organisms expected to be present (e.g. a predisposition towards
325 methanogenic microorganisms). These primers can be used in quantitative PCR (qPCR) for total cell
326 counts, or in sequencing to acquire relative abundance values.

327 Further expanding on the applications of qPCR is the customization of the primers used. While
328 16S rRNA is a universal gene target and been used dating back to 1999 [51], other housekeeping genes
329 specific to a species or interest may be used to get cell counts of targeted populations. For example, the
330 use of primers targeting dissimilatory sulfate reductase, *dsrA,* to monitor sulfate reducing organisms [52]
331 or nitrite reductase, *nirS*, to quantify *Pseudomonas stutzeri* [53], aromatic oxygenases [54]and
332 hydrocarbon hydroxylases [55]. An important consideration when using genes as a cell count proxy is the
333 copy number of the gene in each cell. For 16S rRNA specifically, bacteria can have anywhere from a single
334 copy up to 15, with an average of 3.82 ± 2.61 [56].

Comparison of methods

To compare how the different methods agree with each other, scatter plots were used and linear correlation values were calculated (supplementary Figures 1-6). The R^2 values were calculated for the full datasets of each monitoring method for each species and are reported in Table 4. From these values we can see that the different methods have stronger correlations within certain species, such as *A. woodii,* which has strong correlation between all methods (R^2 = 0.85 – 0.99), while *B. subtilis* has poor correlation across almost all methods where R^2 values range from 0.41 to 0.79 (with the exception of DNA vs. 16S rRNA, R^2 = 0.96). Other species show a strong correlation between some methods such as OD_{600} vs. DNA (*G. subterraneus,* R^2 = 0.98) but poor correlation with others (OD_{600} vs. ATP, R^2 =0.06, and ATP vs. DNA R^2 = 0.02).

Table 4. Linear correlation* values determined from scatter plots of each growth monitoring technique

Species	OD_{600} vs ATP	OD_{600} vs DNA	OD_{600} vs 16S	ATP (ME/mL) vs DNA	ATP (ME/mL) vs 16S	DNA vs 16S
A. woodii	0.94	0.93	0.96	0.85	0.87	0.99
B. subtilis	0.79	0.71	0.74	0.41	0.44	0.96
D. vulgaris	0.43	0.87	0.55	0.55	0.25	0.38
G. subterraneus	0.06	0.98	0.97	0.02	0.02	1.00
P. putida	0.96	0.99	0.51	0.97	0.54	0.59
T. aromatica	0.94	0.81	0.90	0.79	0.84	0.97
Average	0.69	0.88	0.77	0.60	0.49	0.82

*Reported as the R^2 value from XY scatter plots of each data set against each other.

348

349 After converting to microbial equivalents (ME), the ATP measurements follow very similar trends
350 as the OD_{600} readings (average $R^2 = 0.69$, Table 4). The most marked differences in the ATP compared to
351 the OD_{600} graphs occurs in *D. vulgaris* ($R^2 = 0.43$) and *G. subterraneus* ($R^2 = 0.06$) where the shapes of the
352 curves are significantly different owing to the peak in ATP occurring before the stationary phase.
353 Comparing the OD_{600} and ATP values for *A. woodii* ($R^2 = 0.94$), *B. subtilis* ($R^2 = 0.79$), *P. putida* ($R^2 = 0.96$)
354 and *T. aromatica* ($R^2 = 0.94$), we see a strong correlation with slight variations and more variability in the
355 ATP values than seen in OD_{600}. These data agree with the observation that the amount of ATP is consistent
356 at all stages of growth curve [46], while the *D. vulgaris* and *G. subterraneus* datasets disrupt the expected
357 sigmoidal growth curve and shows ATP concentrations are highest during mid log phase, indicating this
358 isn't a universal rule. This is further exemplified in the *G. subterraneus* dataset, whose ATP values were
359 markedly different from other approaches, and correspondingly the linear correlations with ATP are all
360 very low (OD_{600} vs. ATP $R^2 = 0.06$; ATP vs. DNA $R^2 = 0.02$; and ATP vs. 16S $R^2 = 0.02$).

361 The trends in the DNA concentrations closely follow the OD_{600} trends (average $R^2 = 0.88$, Table 4),
362 but have more variance between replicates, possibly owing to the DNA extraction and recovery
363 procedure. As with the DNA concentrations, the trends of the 16S rRNA copy numbers closely followed
364 the OD_{600} readings (average $R^2 = 0.77$) but have a lower linear correlation due to the increased variability
365 between 16S rRNA replicates. Unsurprisingly, DNA vs. 16S rRNA had a strong correlation (average $R^2 =$
366 0.82), but the strongest correlation between any two methods is the OD_{600} and DNA (average $R^2 = 0.88$).
367 The DNA vs. 16S correlation value is dropped by the high variability of the 16S rRNA copies for the final
368 time point of *D. vulgaris*, but with this final time point removed the average R^2 value improves to 0.91
369 (data not shown). The *P. putida* 16S rRNA vs. DNA correlation is also poor but this is again owing to the
370 variability of the replicates for 16S rRNA during the stationary phase. ATP vs. 16S rRNA methods had the

lowest correlation on average between the six pure cultures with an average R^2 value of 0.49 (Table 4), which was mirrored in the correlation between DNA vs. ATP (average R^2 = 0.60, Table 4).

From these comparisons, we can see that both ATP vs. 16S rRNA and ATP vs. DNA concentrations have poor correlation with each other. However, the R^2 values of these averages is skewed downwards as a result of the extremely poor values of *G. subterraneus.* With those values removed, the R^2 values improve to 0.71 for ATP vs. DNA and 0.59 for ATP vs. 16S rRNA. It is tempting to consider the R^2 values with the omissions of the *G. subterraneus*, however they provide a realistic comparison of the diversity of values one might expect in an environmental sample, even in such a small pool as the six species chosen here.

Direct comparison of cell counts

For direct comparisons, we shall look at three time points for each species, chosen to reflect the initial time point (T = 0 hours), mid-log phase (variable) and stationary phase (variable) for each species. For easier direct comparison, all testing methods have been calculated into their unique cells mL^{-1} (Table 5). CFU calculations from all four monitoring methods showed variability of a magnitude lower than the reading, however and on occasion the same order of magnitude or in the case of OD_{600} two orders below. Comparing across the ATP, DNA and 16S rRNA measurements, the ATP microbial equivalents are an order of magnitude or two below calculated DNA and 16S rRNA values. Looking at a single measurement type of a single species, the change between the initial time point to the stationary phase is typically an order of magnitude regardless of the monitoring method. *B. subtilis* had the largest discrepancies between DNA and 16S rRNA calculated cell counts, varying by an order of magnitude. The lowest calculated cell count from all species along all time points is the microbial equivalents of *B. subtilis* at T = 0 hours, which was three to four orders of magnitude below other methods but the discrepancy was closed by mid log phase

and was similar to the calculated values of the other methods and species (Table 5). Stationary phases for DNA and 16S rRNA plateaued primarily at $10^{9\text{-}10}$ cells mL^{-1} (*B. subtilis* 16S rRNA being the exception at 8.4 x 10^8 cells/mL). ATP and OD_{600} values plateaued at $10^{7\text{-}8}$ CFU/mL with the single exception of *A. woodii* ATP value (1.45 x 10^9 ME/mL). This indicates that following these calculations, DNA and 16S rRNA calculations will likely overestimate cell counts compared to OD_{600} and ATP.

Table 5. Summary of the calculated cell counts per milliliter from each monitoring method at the initial time point, mid log phase and stationary phase for all species tested

Species	Time point (hours)	Testing method			
		Converted CFU/mL from OD_{600}	ATP (ME/mL)	Calculated cells from DNA (cells/mL)	Calculated cells from 16S rRNA (cells/mL)
A. woodii	0	4.55 x 10^7 ± 6.60 x 10^5	8.77 x 10^7 ± 8.29 x 10^6	3.02 x 10^8 ± 2.16 x 10^7	1.45 x 10^8 ± 3.48 x 10^7
	13	9.77 x 10^7 ± 8.77 x 10^6	2.74 x 10^8 ± 7.05 x 10^7	3.99 x 10^9 ± 6.71 x 10^8	1.42 x 10^9 ± 1.96 x 10^8
	32	2.63 x 10^8 ± 1.12 x 10^7	1.45 x 10^9 ± 3.74 x 10^8	1.18 x 10^{10} ± 1.35 x 10^9	3.41 x 10^9 ± 2.92 x 10^8
B. subtilis	0	2.07 x 10^7 ± 4.99 x 10^5	3.23 x 10^4 ± 2.98 x 10^4	2.71 x 10^8 ± 6.29 x 10^7	8.85 x 10^7 ± 1.79 x 10^7
	13	9.57 x 10^7 ± 2.08 x 10^7	2.64 x 10^8 ± 1.08 x 10^8	3.28 x 10^9 ± 1.79 x 10^9	8.44 x 10^8 ± 3.79 x 10^8

	30	$8.03 \times 10^7 \pm 4.76 \times 10^6$	$2.30 \times 10^8 \pm 5.61 \times 10^7$	$4.98 \times 10^9 \pm 2.40 \times 10^9$	$8.40 \times 10^8 \pm 4.24 \times 10^8$
D. vulgaris	0	$3.03 \times 10^8 \pm 2.26 \times 10^7$	$5.59 \times 10^6 \pm 9.61 \times 10^4$	$7.32 \times 10^9 \pm 8.65 \times 10^9$	$7.24 \times 10^8 \pm 3.32 \times 10^8$
	28	$3.54 \times 10^8 \pm 3.88 \times 10^7$	$2.00 \times 10^8 \pm 4.28 \times 10^7$	$1.08 \times 10^9 \pm 2.41 \times 10^8$	$4.08 \times 10^9 \pm 8.04 \times 10^8$
	48	$4.06 \times 10^8 \pm 2.96 \times 10^7$	$1.53 \times 10^8 \pm 5.43 \times 10^7$	$1.78 \times 10^{10} \pm 1.10 \times 10^9$	$9.08 \times 10^9 \pm 1.93 \times 10^9$
G. subterraneus	0	$2.71 \times 10^7 \pm 9.43 \times 10^4$	$8.15 \times 10^7 \pm 8.02 \times 10^6$	$2.23 \times 10^9 \pm 2.24 \times 10^8$	$3.77 \times 10^9 \pm 4.51 \times 10^8$
	12	$4.41 \times 10^7 \pm 2.19 \times 10^6$	$2.41 \times 10^8 \pm 8.28 \times 10^7$	$6.00 \times 10^9 \pm 7.82 \times 10^8$	$6.12 \times 10^9 \pm 6.02 \times 10^8$
	32	$6.74 \times 10^7 \pm 4.81 \times 10^6$	$9.16 \times 10^7 \pm 1.75 \times 10^7$	$1.43 \times 10^{10} \pm 2.95 \times 10^9$	$1.17 \times 10^{10} \pm 2.62 \times 10^9$
P. putida	0	$2.58 \times 10^7 \pm 1.63 \times 10^5$	$4.12 \times 10^7 \pm 2.55 \times 10^6$	$2.09 \times 10^9 \pm 1.21 \times 10^8$	$4.29 \times 10^8 \pm 1.47 \times 10^8$
	6	$1.09 \times 10^8 \pm 1.61 \times 10^7$	$5.77 \times 10^8 \pm 1.08 \times 10^8$	$2.47 \times 10^{10} \pm 5.26 \times 10^9$	$7.96 \times 10^9 \pm 2.59 \times 10^9$
	33.5	$2.04 \times 10^8 \pm 4.39 \times 10^7$	$8.65 \times 10^8 \pm 1.46 \times 10^8$	$3.99 \times 10^{10} \pm 9.48 \times 10^9$	$4.79 \times 10^9 \pm 1.55 \times 10^9$
T. aromatica	0	$3.35 \times 10^7 \pm 1.39 \times 10^6$	$5.81 \times 10^7 \pm 2.97 \times 10^6$	$2.90 \times 10^{10} \pm 4.08 \times 10^8$	$7.01 \times 10^8 \pm 2.83 \times 10^8$

	20	$1.45 \times 10^8 \pm 6.38 \times 10^6$	$3.51 \times 10^8 \pm 2.64 \times 10^7$	$6.11 \times 10^8 \pm 1.11 \times 10^8$	$1.41 \times 10^{10} \pm 7.54 \times 10^9$
	48	$1.65 \times 10^8 \pm 2.30 \times 10^6$	$4.41 \times 10^8 \pm 2.90 \times 10^7$	$1.41 \times 10^{10} \pm 1.53 \times 10^9$	$2.62 \times 10^{10} \pm 7.66 \times 10^9$

Conclusion

This work set out to compare monitoring techniques readily employed in the field and compare them to methods best suited for lab cultures. OD_{600} is poorly suited for field samples due to the requirement for a liquid medium and the presence of non-biological materials frequently present in environmental samples which will artificially increase OD_{600} values. This is illustrated by the *D. vulgaris* dataset, where the scattering of light is increased due to the precipitation of iron sulfide resulting from sulfide production by *D. vulgaris*. Even without the presence of a precipitate in the media, direct OD_{600} comparisons have little value such as with *G. subterraneus,* where OD_{600} values peaked at 0.317 while the other species reached readings of 1.001 and 1.296 in the stationary phase (*P. putida* and *A. woodii* respectively). As a result, OD_{600} is only suited for rapid monitoring of a pure culture and has no value for cross comparisons.

As shown in Table 5, the trends are consistent but the actual converted cell counts can vary on the order of magnitudes. This indicates that while any single method can be used with reasonable confidence to assess the microbial cell density in a particular system or environment, comparing multiple methods will lead to false assumptions regarding changes in cell concentrations.

Due to the need of including additional values for converting ATP, 16S rRNA copy numbers and DNA into cell count equivalents, it is more reasonable to leave these readings as their true output (i.e. pg ATP, copy number 16S rRNA and µg DNA respectively) rather than adding converting values using equations containing general assumptions, which certainly can skew output values, especially in mixed environmental samples where the factors (e.g. DNA amount per cell) may vary between species.

This work shows that using DNA concentrations as a proxy for cell counts could be considered the best universal indicator for microbial cells numbers. It carries a strong correlation to OD_{600} values in pure cultures in liquid media, is not as susceptible to large variation between replicates as 16S rRNA qPCR and theoretically isn't overly susceptible to calculation bias as the range of DNA concentrations within a single cell is 1.6-2.4 fg [33]. Using DNA as a cell count proxy has the only reproducible DNA recovery as a potential issue, where Gram positive cells may not lyse as easily as Gram negative cells in which case DNA concentrations may underestimate the total cell counts.

While this work focused on pure cultures of diverse environmental strains, we believe these results can be extrapolated to mixed species and field samples with highly diverse microbial populations. The simplest and most impactful conclusion from this is that there is no true, or best method for monitoring microbial growth, rather being consistent with a monitoring technique is the most important factor and to understand the used approaches limitations as illustrated here.

References

1. Madigan MT, Bender KS, Buckley DH, Sattley WM, Stahl DA. Brock Biology of Microorganisms. 15th ed. Harlow, United Kingdom: Pearson Education; 2019. 1 online resource (1064 pages) : illustrations.

2. Colwell RR, Brayton PR, Grimes DJ, Roszak DB, Huq SA, Palmer LM. Viable but Non-Culturable Vibrio cholerae and Related Pathogens in the Environment: Implications for Release of Genetically Engineered Microorganisms. Bio/Technology. 1985;3(9):817–20. DOI: 10.1038/nbt0985-817

3. Byrd JJ, Xu HS, Colwell RR. Viable but nonculturable bacteria in drinking water. Appl Environ Microbiol. 1991;57(3):875–8. DOI: 10.1128/AEM.57.3.875-878.1991

4. Xu H, Roberts N, Singleton F, Attwell R, Grimes D, Colwell R. Survival and viability of nonculturableEscherichia coli andVibrio cholerae in the estuarine and marine environment. Microb Ecol. 1982;8:313–23.

5. Razban B, Nelson KY, Cullimore DR, Cullimore J, McMartin DW. Quantitative bacteriological assessment of aerobic wastewater treatment quality and plant performance. J Environ Sci Heal Part A. 2012;47(5):727–33. DOI: 10.1080/10934529.2012.660093

6. Sharpe AN, Michaud GL. Enumeration of High Numbers of Bacteria Using Hydrophobic Grid-Membrane Filters. Appl Microbiol. 1975;30(4):519–24. DOI: 10.1128/AM.30.4.519-524.1975

7. Tawakoli PN, Al-Ahmad A, Hoth-Hannig W, Hannig M, Hannig C. Comparison of different live/dead stainings for detection and quantification of adherent microorganisms in the initial oral biofilm. Clin Oral Investig. 2012;17(3):841–50. DOI: 10.1007/S00784-012-0792-3

8. Hannig C, Hannig M, Rehmer O, Braun G, Hellwig E, Al-Ahmad A. Fluorescence microscopic visualization and quantification of initial bacterial colonization on enamel in situ. Arch Oral Biol. 2007;52(11):1048–56. DOI: 10.1016/J.ARCHORALBIO.2007.05.006

9. Djordjevic D, Wiedmann M, McLandsborough LA. Microtiter plate assay for assessment of Listeria monocytogenes biofilm formation. Appl Environ Microbiol. 2002;68(6):2950–8. DOI: 10.1128/AEM.68.6.2950-2958.2002

10. Bhupathiraju VK, Hernandez M, Krauter P, Alvarez-Cohen L. A new direct microscopy based method for evaluating in-situ bioremediation. J Hazard Mater. 1999;67:299–312.

11. Harmsen HJM, Wildeboer-Veloo ACM, Grijpstra J, Knol J, Degener JE, Welling GW. Development of 16S rRNA-based probes for the Coriobacterium group and the Atopobium cluster and their application for enumeration of Coriobacteriaceae in human feces from volunteers of different age groups. Appl Environ Microbiol. 2000;66(10):4523–7. DOI: 10.1128/AEM.66.10.4523-4527.2000

12. Langendijk PS, Schut F, Jansen GJ, Raangs GC, Kamphuis GR, Wilkinson MHF, et al. Quantitative fluorescence in situ hybridization of Bifidobacterium spp. with genus-specific 16S rRNA-targeted probes and its application in fecal samples. Appl Environ Microbiol. 1995;61(8):3069–75. DOI: 10.1128/AEM.61.8.3069-3075.1995

13. Jian C, Luukkonen P, Yki-Järvinen H, Salonen A, Korpela K. Quantitative PCR provides a simple and accessible method for quantitative microbiota profiling. PLoS One. 2020;15(1):e0227285. DOI: 10.1371/JOURNAL.PONE.0227285

14. Smith CJ, Nedwell DB, Dong LF, Osborn AM. Evaluation of quantitative polymerase chain reaction-based approaches for determining gene copy and gene transcript numbers in

environmental samples. Environ Microbiol. 2006;8(5):804–15. DOI: 10.1111/J.1462-2920.2005.00963.X

15. Suzuki MT, Taylor LT, DeLong EF. Quantitative analysis of small-subunit rRNA genes in mixed microbial populations via 5'-nuclease assays. Appl Environ Microbiol. 2000;66(11):4605–14. DOI: 10.1128/AEM.66.11.4605-4614.2000

16. Breznak JA, Costilow RN. Physicochemical Factors in Growth. In: Methods for General and Molecular Microbiology. Washington, DC, USA: ASM Press; 2014. p. 309–29. DOI: 10.1128/9781555817497.ch14

17. Hungate RE. Chapter IV A Roll Tube Method for Cultivation of Strict Anaerobes. Methods Microbiol. 1969;3(PART B):117–32. DOI: 10.1016/S0580-9517(08)70503-8

18. Hungate RE. The Anaerobic Mesophilic Cellulolytic Bacteria. Bacteriol Rev. 1950;14(1):1.

19. Balch W, Wolfe R. New approach to the cultivation of methanogenic bacteria: 2-mercaptoethanesulfonic acid (HS-CoM)-dependent growth of Methanobacterium ruminantium in a pressureized atmosphere. Appl Environ Microbiol. 1976;32(6):781–91. DOI: 10.1128/AEM.32.6.781-791.1976

20. Chan ECS, Siboo R, Touyz LZG, Qiu Y-S, Klitorinos A. A successful method for quantifying viable oral anaerobic spirochetes. Oral Microbiol Immunol. 1993;8(2):80–3. DOI: 10.1111/J.1399-302X.1993.TB00549.X

21. Martins CHG, Carvalho TC, Souza MGM, Ravagnani C, Peitl O, Zanotto ED, et al. Assessment of antimicrobial effect of Biosilicate® against anaerobic, microaerophilic and facultative anaerobic microorganisms. J Mater Sci Mater Med. 2011;22(6):1439–46. DOI: 10.1007/S10856-011-4330-7

22. Salanitro JP, Fairchilds IG, Zgornicki YD. Isolation, Culture Characteristics, and Identification of

Anaerobic Bacteria from the Chicken Cecum. Appl Microbiol. 1974;27(4):678–87. DOI: 10.1128/AM.27.4.678-687.1974

23. Montero B, Garcia-Morales JL, Sales D, Solera R. Evolution of microorganisms in thermophilic-dry anaerobic digestion. Bioresour Technol. 2008;99(8):3233–43. DOI: 10.1016/J.BIORTECH.2007.05.063

24. Himmelberg AM, Brüls T, Farmani Z, Weyrauch P, Barthel G, Schrader W, et al. Anaerobic degradation of phenanthrene by a sulfate-reducing enrichment culture. Environ Microbiol. 2018;20(10):3589–600. DOI: 10.1111/1462-2920.14335

25. Pronk JT, De Bruyn JC, Bos P, Kuenen JG. Anaerobic growth of Thiobacillus ferrooxidans. Appl Environ Microbiol. 1992;58(7):2227–30. DOI: 10.1128/AEM.58.7.2227-2230.1992

26. Mauerhofer LM, Pappenreiter P, Paulik C, Seifert AH, Bernacchi S, Rittmann SKMR. Methods for quantification of growth and productivity in anaerobic microbiology and biotechnology. Folia Microbiol (Praha). 2019;64(3):321–60. DOI: 10.1007/s12223-018-0658-4

27. Ramos-Padrón E, Bordenave S, Lin S, Bhaskar IM, Dong X, Sensen CW, et al. Carbon and Sulfur Cycling by Microbial Communities in a Gypsum-Treated Oil Sands Tailings Pond. Environ Sci Technol. 2010;45(2):439–46. DOI: 10.1021/ES1028487

28. Stams AJM, Sousa DZ, Kleerebezem R, Plugge CM. Role of syntrophic microbial communities in high-rate methanogenic bioreactors. Water Sci Technol. 2012;66(2):352–62. DOI: 10.2166/WST.2012.192

29. Monod J. The Growth of Bacterial Cultures. Ann Rev Microbiol. 1949;3(1):371–94. DOI: 10.1146/ANNUREV.MI.03.100149.002103

30. Maloney LC, Nelson YM, Kitts CL. Characterization of aerobic and anaerobic microbial activity in

hydrocarbon-contaminated soil. In: Gavaskar A, Chen A, editors. Remediation of Chlorinated and Recalcitrant Compounds - 2004. Battelle Press; 2004. p. 3E – 02.

31. Manti A, Boi P, Falcioni T, Canonico B, Ventura A, Sisti D, et al. Bacterial cell monitoring in wastewater treatment plants by flow cytometry. Water Environ Res. 2008;80(4):346–54. DOI: 10.2175/106143007X221418

32. Caporaso JG, Lauber CL, Walters WA, Berg-Lyons D, Lozupone CA, Turnbaugh PJ, et al. Global patterns of 16S rRNA diversity at a depth of millions of sequences per sample. Proc Natl Acad Sci. 2011;108(Supplement_1):4516–22. DOI: 10.1073/pnas.1000080107

33. Bakken LR, Olsen RA. DNA-content of soil bacteria of different cell size. Soil Biol Biochem. 1989;21(6):789–93. DOI: 10.1016/0038-0717(89)90172-7

34. Kim D-J, Chung S-G, Lee S-H, Choi J-W. Relation of microbial biomass to counting units for Pseudomonas aeruginosa. African J Microbiol Res. 2012;6(21):4620–2. DOI: 10.5897/AJMR10.902

35. Bracho M, Araujo I, de Romero M, Ocando L, García M, Sarró MI, et al. Comparison Of Bacterial Growth Of Sulfate Reducing Bacteria Evaluated By Serial Dilution, Pure Plate And Epifluorescence Techniques. In: CORROSION 2007. OnePetro; 2007. p. NACE-07530.

36. Myers JA, Curtis BS, Curtis WR. Improving accuracy of cell and chromophore concentration measurements using optical density. BMC Biophys. 2013;6(1):4. DOI: 10.1186/2046-1682-6-4

37. Snellen JE, Marr AG, Starr MP. A membrane filter direct count technique for enumerating Bdellovibrio. Curr Microbiol. 1978;1(2):117–22. DOI: 10.1007/BF02605428

38. Duncan CL. Time of enterotoxin formation and release during sporulation of Clostridium perfringens type A. J Bacteriol. 1973;113(2):932–6. DOI: 10.1128/JB.113.2.932-936.1973

544 39. Xu Z, Liang Y, Lin S, Chen D, Li B, Li L, et al. Crystal Violet and XTT Assays on Staphylococcus
545 aureus Biofilm Quantification. Curr Microbiol. 2016;73(4):474–82. DOI: 10.1007/s00284-016-
546 1081-1

547 40. Ommen P, Zobek N, Meyer RL. Quantification of biofilm biomass by staining: Non-toxic safranin
548 can replace the popular crystal violet. J Microbiol Methods. 2017;141:87–9. DOI:
549 10.1016/j.mimet.2017.08.003

550 41. Vogel C, Marcotte EM. Insights into the regulation of protein abundance from proteomic and
551 transcriptomic analyses. Nat Rev Genet. 2012;13(4):227. DOI: 10.1038/NRG3185

552 42. Frostegård Å, Tunlid A, Bååth E. Microbial biomass measured as total lipid phosphate in soils of
553 different organic content. J Microbiol Methods. 1991;14(3):151–63. DOI: 10.1016/0167-
554 7012(91)90018-L

555 43. Nguyen TDP, Nguyen DH, Lim JW, Chang C-K, Leong HY, Tran TNT, et al. Investigation of the
556 Relationship between Bacteria Growth and Lipid Production Cultivating of Microalgae Chlorella
557 Vulgaris in Seafood Wastewater. Energies. 2019;12(12):2282. DOI: 10.3390/EN12122282

558 44. Neubauer C, Kasi AS, Grahl N, Sessions AL, Kopf SH, Kato R, et al. Refining the application of
559 microbial lipids as tracers of Staphylococcus aureus growth rates in cystic fibrosis sputum. J
560 Bacteriol. 2018;200(24). DOI: 10.1128/JB.00365-18

561 45. Hattori N, Sakakibara T, Kajiyama N, Igarashi T, Maeda M, Murakami S. Enhanced microbial
562 biomass assay using mutant luciferase resistant to benzalkonium chloride. Anal Biochem.
563 2003;319(2):287–95. DOI: 10.1016/S0003-2697(03)00322-1

564 46. Schneider DA, Gourse RL. Relationship between growth rate and ATP concentration in
565 escherichia coli: A bioassay for available cellular ATP. J Biol Chem. 2004;279(9):8262–8. DOI:

10.1074/jbc.M311996200

47. Soini J, Falschlehner C, Mayer C, Böhm D, Weinel S, Panula J, et al. Transient increase of ATP as a response to temperature up-shift in Escherichia coli. Microb Cell Fact. 2005;4(1):9. DOI: 10.1186/1475-2859-4-9

48. Cai L, Ye L, Tong AHY, Lok S, Zhang T. Biased Diversity Metrics Revealed by Bacterial 16S Pyrotags Derived from Different Primer Sets. PLoS One. 2013;8(1):e53649. DOI: 10.1371/JOURNAL.PONE.0053649

49. Walker AW, Martin JC, Scott P, Parkhill J, Flint HJ, Scott KP. 16S rRNA gene-based profiling of the human infant gut microbiota is strongly influenced by sample processing and PCR primer choice. Microbiome 2015 31. 2015;3(1):1–11. DOI: 10.1186/S40168-015-0087-4

50. Baker GC, Smith JJ, Cowan DA. Review and re-analysis of domain-specific 16S primers. J Microbiol Methods. 2003;55(3):541–55. DOI: 10.1016/j.mimet.2003.08.009

51. Edgcomb V, McDonald J, Devereux R, Smith D. Estimation of bacterial cell numbers in humic acid-rich salt marsh sediments with probes directed to 16S ribosomal DNA. Appl Environ Microbiol. 1999;65(4):1516–23. DOI: 10.1128/AEM.65.4.1516-1523.1999

52. Müller AL, Kjeldsen KU, Rattei T, Pester M, Loy A. Phylogenetic and environmental diversity of DsrAB-type dissimilatory (bi)sulfite reductases. ISME J. 2015;9(5):1152–65. DOI: 10.1038/ismej.2014.208

53. Grüntzig V, Nold SC, Zhou J, Tiedje JM. Pseudomonas stutzeri nitrite reductase gene abundance in environmental samples measured by real-time PCR. Appl Environ Microbiol. 2001;67(2):760–8. DOI: 10.1128/AEM.67.2.760-768.2001

54. Baldwin BR, Nakatsu CH, Nies L. Detection and enumeration of aromatic oxygenase genes by

multiplex and real-time PCR. Appl Environ Microbiol. 2003;69(6):3350–8. DOI: 10.1128/AEM.69.6.3350-3358.2003

55. McKew BA, Coulon F, Yakimov MM, Denaro R, Genovese M, Smith CJ, et al. Efficacy of intervention strategies for bioremediation of crude oil in marine systems and effects on indigenous hydrocarbonoclastic bacteria. Environ Microbiol. 2007;9(6):1562–71. DOI: 10.1111/J.1462-2920.2007.01277.X

56. Sun DL, Jiang X, Wu QL, Zhou NY. Intragenomic heterogeneity of 16S rRNA genes causes overestimation of prokaryotic diversity. Appl Environ Microbiol. 2013;79(19):5962–9. DOI: 10.1128/AEM.01282-13

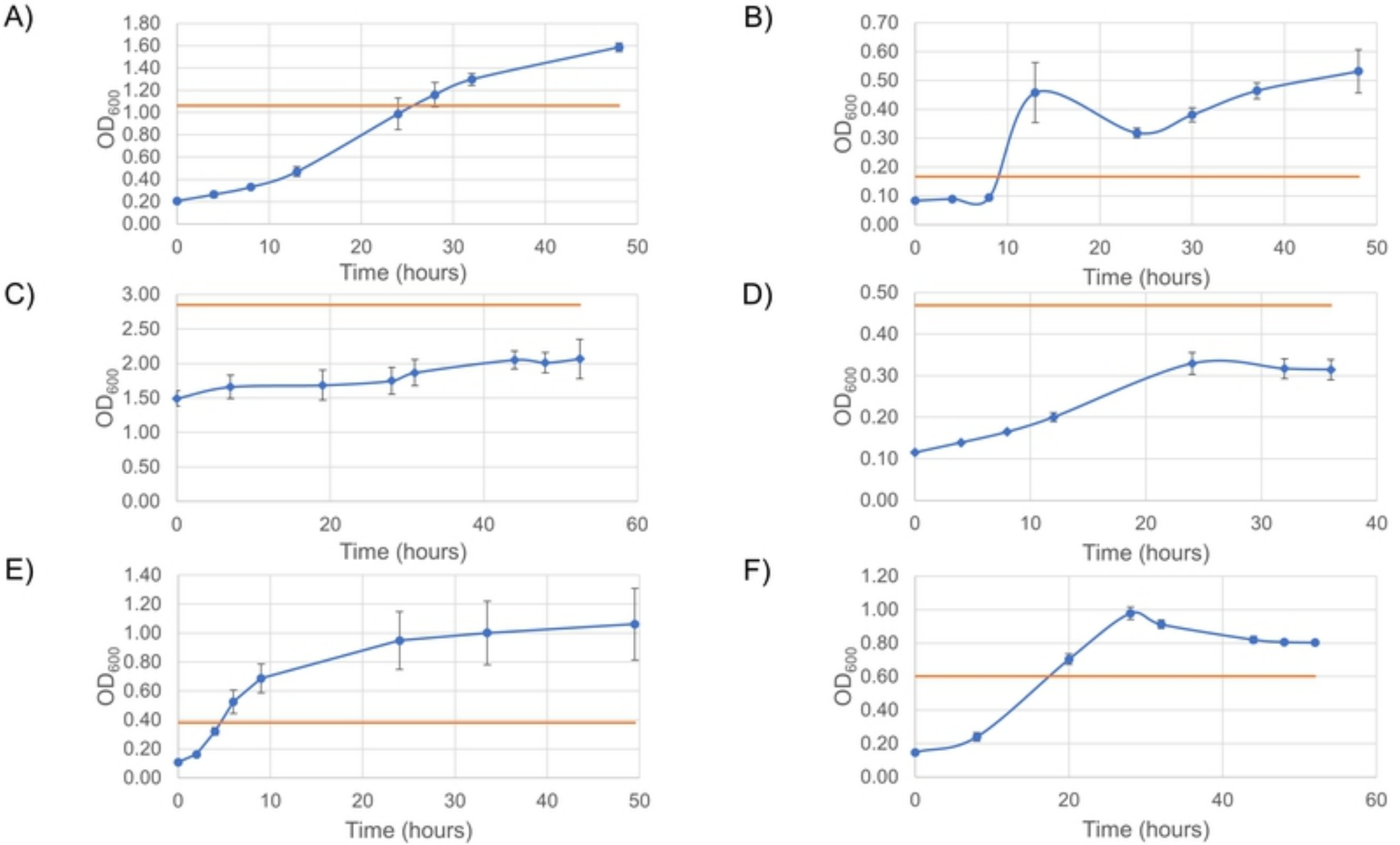

Figure

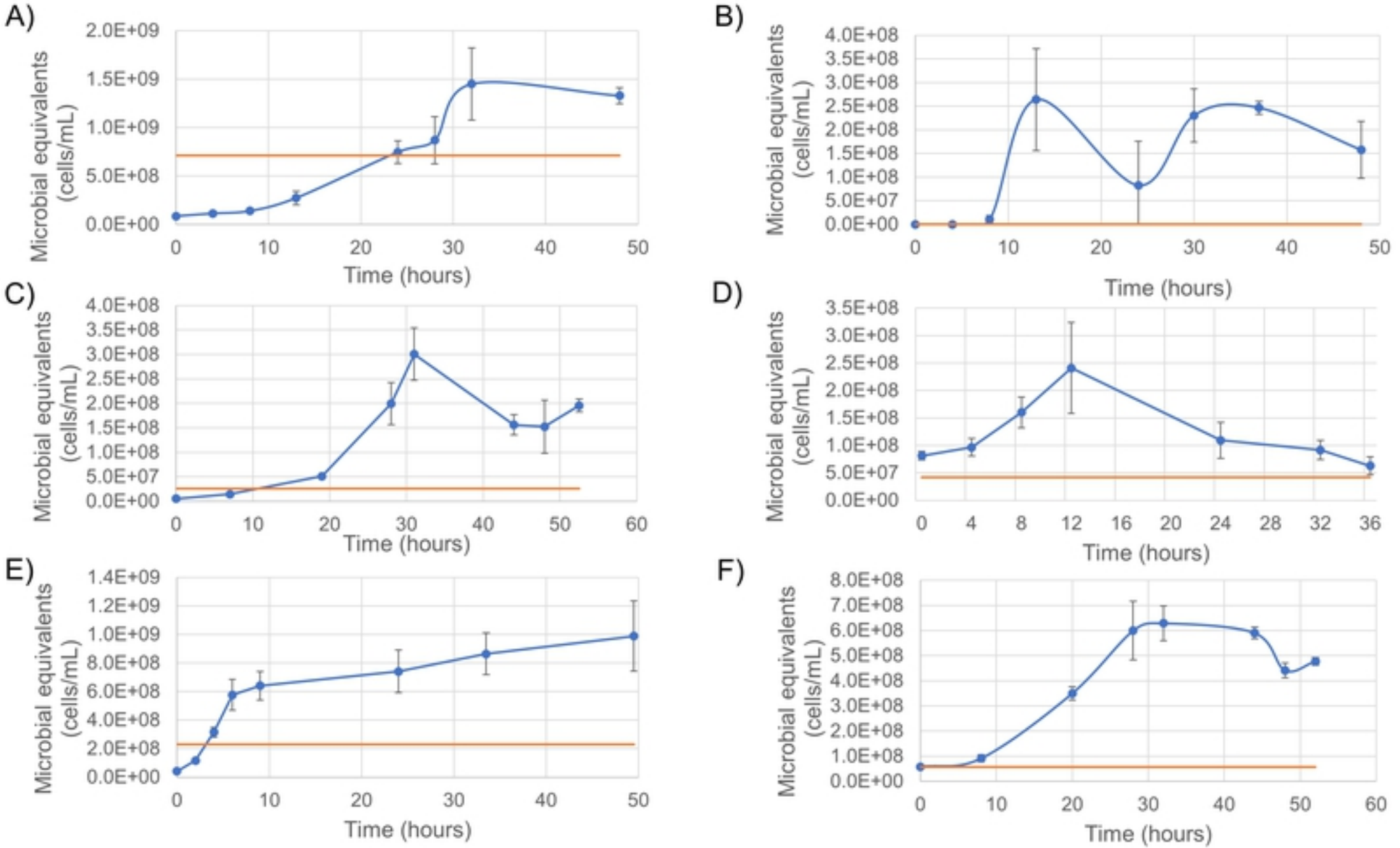
A)
Microbial equivalents (cells/mL)
2.0E+09
1.5E+09
1.0E+09
5.0E+08
0.0E+00
0
10
20
30
40
50
Time (hours)
B)
Microbial equivalents (cells/mL)
4.0E+08
3.5E+08
3.0E+08
2.5E+08
2.0E+08
1.5E+08
1.0E+08
5.0E+07
0.0E+00
0
10
20
30
40
50
Time (hours)
C)
Microbial equivalents (cells/mL)
4.0E+08
3.5E+08
3.0E+08
2.5E+08
2.0E+08
1.5E+08
1.0E+08
5.0E+07
0.0E+00
0
10
20
30
40
50
60
Time (hours)
D)
Microbial equivalents (cells/mL)
3.5E+08
3.0E+08
2.5E+08
2.0E+08
1.5E+08
1.0E+08
5.0E+07
0.0E+00
0
4
8
12
16
20
24
28
32
36
Time (hours)
E)
Microbial equivalents (cells/mL)
1.4E+09
1.2E+09
1.0E+09
8.0E+08
6.0E+08
4.0E+08
2.0E+08
0.0E+00
0
10
20
30
40
50
Time (hours)
F)
Microbial equivalents (cells/mL)
8.0E+08
7.0E+08
6.0E+08
5.0E+08
4.0E+08
3.0E+08
2.0E+08
1.0E+08
0.0E+00
0
10
20
30
40
50
60
Time (hours)

Figure

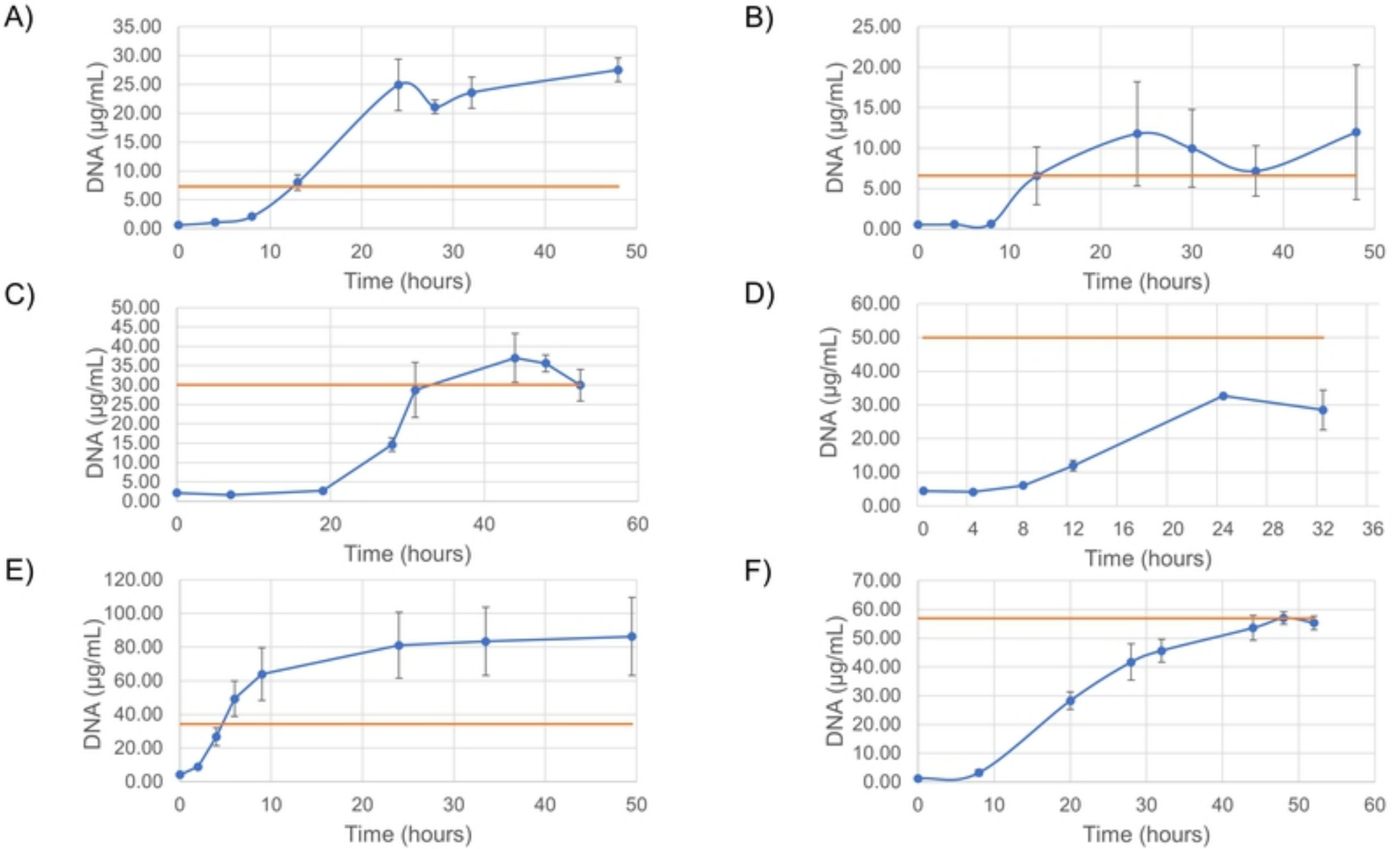
A)
DNA (µg/mL)
Time (hours)
B)
DNA (µg/mL)
Time (hours)
C)
DNA (µg/mL)
Time (hours)
D)
DNA (µg/mL)
Time (hours)
E)
DNA (µg/mL)
Time (hours)
F)
DNA (µg/mL)
Time (hours)

Figure

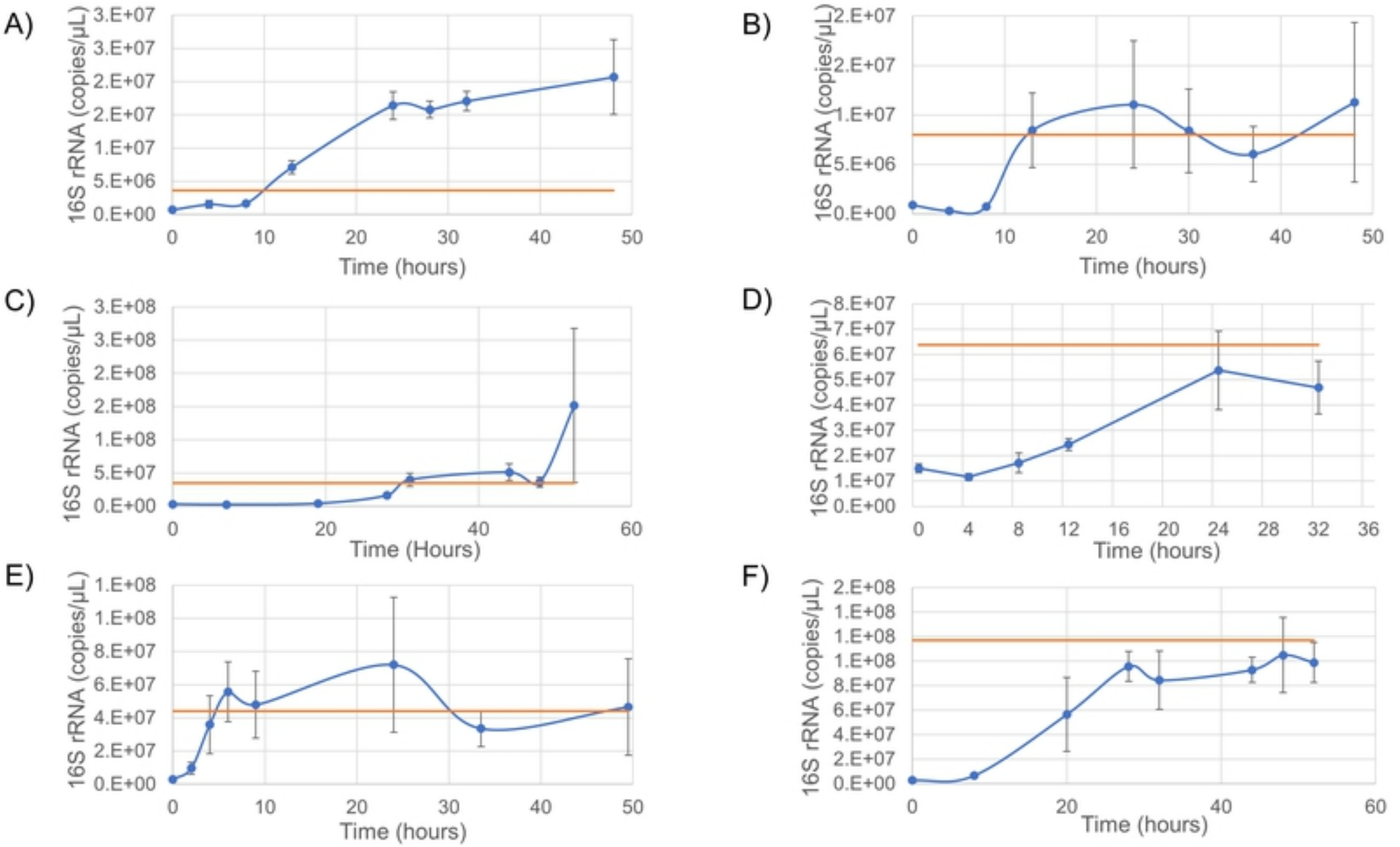
A)
16S rRNA (copies/µL)
3.E+07
3.E+07
2.E+07
2.E+07
1.E+07
5.E+06
0.E+00
0
10
20
30
40
50
Time (hours)
B)
16S rRNA (copies/µL)
2.E+07
2.E+07
1.E+07
5.E+06
0.E+00
0
10
20
30
40
50
Time (hours)
C)
16S rRNA (copies/µL)
3.E+08
3.E+08
2.E+08
2.E+08
1.E+08
5.E+07
0.E+00
0
20
40
60
Time (Hours)
D)
16S rRNA (copies/µL)
8.E+07
7.E+07
6.E+07
5.E+07
4.E+07
3.E+07
2.E+07
1.E+07
0.E+00
0
4
8
12
16
20
24
28
32
36
Time (hours)
E)
16S rRNA (copies/µL)
1.E+08
1.E+08
8.E+07
6.E+07
4.E+07
2.E+07
0.E+00
0
10
20
30
40
50
Time (hours)
F)
16S rRNA (copies/µL)
2.E+08
1.E+08
1.E+08
1.E+08
8.E+07
6.E+07
4.E+07
2.E+07
0.E+00
0
20
40
60
Time (hours)

Figure